Journal of Solid State Chemistry 183 (2010) 1733–1739

Contents lists available at ScienceDirect

Journal of Solid State Chemistry

journal homepage: www.elsevier.com/locate/jssc

Effects of gold catalysts and thermal evaporation method modifications on the growth process of $Zn_{1-x}Mg_xO$ nanowires

Ramin Yousefi [a,b,*], Muhamad Rasat Muhamad [a]

[a] Solid State Laboratory, Department of Physics, University of Malaya, 50603 Kuala Lumpur, Malaysia
[b] Department of Physics, Islamic Azad University, Masjed-Soleiman Branch, Masjed-Soleiman, Iran

ARTICLE INFO

Article history:
Received 5 November 2009
Received in revised form
2 May 2010
Accepted 7 May 2010
Available online 24 May 2010

Keywords:
$Zn_{1-x}Mg_xO$ nanowires
Thermal evaporation
Fick's first law
Photoluminescence
Raman

ABSTRACT

In this paper, we investigate the roles of gold catalysts and thermal evaporation method modifications in the growth process of $Zn_{1-x}Mg_xO$ nanowires. $Zn_{1-x}Mg_xO$ nanowires are fabricated on silicon substrates with and without using a gold catalyst. Characterizations reveal that Mg acts in a self-catalyst role during the growth process of $Zn_{1-x}Mg_xO$ nanowires grown on catalyst-free substrate. The optical properties and crystalline quality of the $Zn_{1-x}Mg_xO$ nanowires are characterized by room temperature photoluminescence (PL) measurements and Raman spectroscopy, respectively. The Raman and PL studies demonstrate that the $Zn_{1-x}Mg_xO$ nanowires grown using the catalyst-free method have good crystallinity with excellent optical properties and have a larger band-gap in comparison to those grown with the assistance of gold.

1. Introduction

ZnO is an important wide-band-gap semiconductor with a direct band-gap of 3.37 eV and a high exciton binding energy of 60 meV, which is greater than the thermal energy at room temperature. ZnO is a promising material for ultraviolet nano-optoelectronic devices and lasers operating at room temperature [1]. By alloying ZnO with another material of a different band-gap, the band-gap of ZnO can be fine tuned; thus affecting the wavelength of exciton emission. In addition, alloying ZnO with MgO or Mg creates $Zn_{1-x}Mg_xO$, which is a potential candidate for future optoelectronic devices. The addition of MgO, which has a larger band-gap (7.7 eV) than ZnO, results in a widened band-gap. Additionally, MgO has less lattice mismatch with ZnO as the ionic magnesium and zinc are relatively similar [2–4]. Recently, many papers have reported the formation of $Zn_{1-x}Mg_xO$ nanostructures with different methods such as metal-organic vapor phase deposition [5–11], pulsed laser deposition [12,13], and thermal evaporation [14–24]. However, only a few of these papers reported a very high optical quality of $Zn_{1-x}Mg_xO$ nanostructures, resulting from the strong inclination of magnesium to react with oxygen. The resultant products usually have large oxygen vacancy centers; therefore, the optical efficiency of such products is significantly weak.

Of the various methods available for synthesizing nanowires, thermal evaporation provides a particularly cost effective and high quality equilibrium process, in which the composition of ternary or quaternary nanostructures can be controlled by the content and melting points of the sources used. Therefore, it can see great numbers of publications, which have used this method for growth of ZnO nanostructures, in literature. On the other hand, several papers have reported that $Zn_{1-x}Mg_xO$ nanowires cannot be formed by the thermal evaporation method without the use of Au catalysts on Si substrates. The effects of gold catalysts on the growth process of $Zn_{1-x}Mg_xO$ nanowires were also investigated in our previous work [25]. We observed that a gold catalyst has a dramatic role in the doping of Mg in ZnO nanostructures. [25]. This may be due to a smaller electronegativity difference between Mg and Si ($\zeta_{Si}-\zeta_{Mg}\approx 0.6$) in comparison to that between Mg and Au ($\zeta_{Au}-\zeta_{Mg}\approx 1.3$). A larger electronegativity difference creates a large electric field between the vapors and the nuclei sites on the substrate, which is needed to grow one-dimensional nanostructures by such methods [26].

Based on these reasons, in this paper, the thermal evaporation set-up is modified to increase the Mg concentration in the system. Additionally, the effects of the Au catalyst on the growth process of $Zn_{1-x}Mg_xO$ nanowires are investigated. Here, we defined a mechanism for the growth of $Zn_{1-x}Mg_xO$ nanowires by increasing the Mg concentration in an one-ended tube. The resultant $Zn_{1-x}Mg_xO$ nanowires obtained without the assistance of a gold catalyst. Moreover, the effects of different thicknesses of gold catalysts on the growth process of $Zn_{1-x}Mg_xO$ nanowires are investigated.

* Corresponding author. Fax: +60379674146, +986813330093.
E-mail address: yousefi.ramin@gmail.com (R. Yousefi).

0022-4596/$ - see front matter © 2010 Elsevier Inc. All rights reserved.
doi:10.1016/j.jssc.2010.05.007

2. Experimental

The growth of $Zn_{1-x}Mg_xO$ nanowires was performed in a horizontal tube furnace. This system contains a quartz tube vacuum chamber 100 cm long and 5 cm in diameter. A smaller one-ended quartz tube, 50 cm long, and 2 cm in diameter that contained the precursor materials (ZnO and Mg) and substrate was placed within the vacuum chamber. A mixture of the zinc oxide powder (99.99%) and commercial graphite powder at a 1:1 weight ratio was used as the precursor material of ZnO, and Mg powder (99.99%) was used as the precursor material of Mg ($Mol_{ZnO}/Mol_{Mg}=10:2$). The precursor material of ZnO was placed at the closed end of the smaller quartz tube, while the Mg powder was placed 15 cm away from the ZnO material, and a Si(111) substrate was placed downstream of the precursor materials, as shown in Fig. 1. The small tube was then inserted into the vacuum chamber such that the closed end was at the center of the furnace. The precursor materials of ZnO and Mg were heated up to 950 and 750 °C, respectively, and the temperature of the substrate was maintained at 600 °C during the growth process of the $Zn_{1-x}Mg_xO$ nanowires (Fig. 1). High purity N_2 gas was fed at about 100 sccm into the furnace at one end, while the other end was connected to a rotary pump. The growth process was allowed to proceed for 1 h. A vacuum of 6 Torr was maintained inside the tube furnace during the deposition of the nanostructures. In this manner, three sets of wires made, one using a catalyst-free substrate (sample (a)) and the others using substrates coated with 10-nm (sample (b)) and 30-nm (sample (c)) Au films. Pure ZnO nanowires were also grown under the same conditions using a catalyst-free substrate (sample (d)).

The crystal structure and morphology of the products were investigated by field emission scanning electron microscopy (FESEM, Quanta 200F) and X-ray diffraction (XRD, Siemens D5000). The elemental contents of the products were investigated using energy dispersive X-ray analysis (EDX, Quanta 200F). Room temperature photoluminescence and Raman (Jobin Yvon Horiba HR 800 UV) spectroscopy were employed to study the optical properties and crystallinity of the $Zn_{1-x}Mg_xO$ and pure ZnO nanowires using a He–Cd laser with a wavelength of 325 nm and an Ar ion laser with an emission wavelength of 514.5 nm for PL and Raman measurements, respectively.

3. Results and discussion

Fig. 2(a_1)–(c_1) show low-magnification FESEM images of the $Zn_{1-x}Mg_xO$ nanowires that were grown on the various substrates: without a gold catalyst (sample (a)), with a 10-nm-thick gold film (sample (b)) and with a 30-nm-thick gold film (sample (c)), respectively. Fig. 2(a_2)–(c_2) show high-magnification FESEM images and EDX spectra at different locations along individual $Zn_{1-x}Mg_xO$ nanowires, which were grown on the substrates under different conditions. As can be observed in the FESEM images, the shapes of these nanowires are dramatically different. Fig. 2(a_2) shows a single $Zn_{1-x}Mg_xO$ nanowire with its EDX spectra taken from different places along this nanowire, which was grown on the catalyst-free substrate. A rectangular shape of this nanowire can be clearly seen in Fig. 2(a_2). $Zn_{1-x}Mg_xO$ nanowires with a rectangular shape were also observed in our previous work [25]. It can be seen that, the nanowire is not straight and that it does not have a uniform width for two of the sides along its axis. In addition, the EDX spectra indicate an increase in the percent composition of Mg when moving towards the tip of the nanowire. Fig. 2(b_2) and (c_2) also show individual $Zn_{1-x}Mg_xO$ nanowires with their EDX spectra taken from different places along these nanowires, which were grown on the substrates coated with 10-nm (sample (b)) and 30-nm (sample (c)) Au films, respectively. The shapes of these nanowires are completely different in comparison to the nanowires that were grown on the catalyst-free substrate. As is visible in the FESEM images, the nanowires are completely straight, but are tapered with tip diameters of 10 ± 2 and 80 ± 5 nm and base diameters of 80 ± 5 and 130 ± 10 nm for samples (b) and (c), respectively. By a comparison observation between $Zn_{1-x}Mg_xO$ nanowires, it can be understood that, tapering of the $Zn_{1-x}Mg_xO$ nanowires may be due to the reaction products. In fact, the disturbance of the vapor concentrations in the growth process of $Zn_{1-x}Mg_xO$ nanowires is a major factor that changes the diameter of the catalyst alloy droplets. Furthermore, stability of catalyst alloy droplets during of the growth process is dependent on eutectic point of compounds in alloy droplet [26]. In general, one could expect the formation of Au–Zn, Au–Mg, or Zn–Mg binary alloys, or of a ternary alloy involving all three components. Therefore, the presence of the Mg element may be changed Au–Zn eutectic point during the growth process. As shown in Fig (2), the diameter of the nanowires grown with the 30-nm-thick gold film is larger than the diameter of the nanowires grown with the 10-nm-thick gold film, because the nanowire diameter is known to be dependent on catalyst particle size. The thicker gold film produces larger gold droplets, so the nanowires grown with the thicker gold film have a larger diameter. Based on the results obtained from the EDX spectra of these nanowires, the growth process of these nanowires is determined to be the vapor–liquid–solid (VLS) mechanism [27]. One can clearly observe gold particles at the tips of the nanowires in Fig. 2(c_1) and (c_2). The Mg element is not detected at the nanowire tips that were grown on the substrates coated with Au.

Table 1 shows the average Mg content of $Zn_{1-x}Mg_xO$ nanowires grown on different substrates. It can be clearly seen that the average Mg content of the $Zn_{1-x}Mg_xO$ nanowires grown on the catalyst-free substrate is larger than those grown on the substrates coated with gold films. Moreover this table shows the Mg content at different positions of a single nanowire for three samples: (1) at the tip, (2) in the middle, and (3) at the bottom. It can be observed that the distribution of Mg in the nanowires grown on the catalyst-free substrate is significantly different from that of the other nanowires, which were grown on substrates coated with Au. Additionally, samples (b) and (c) show that the

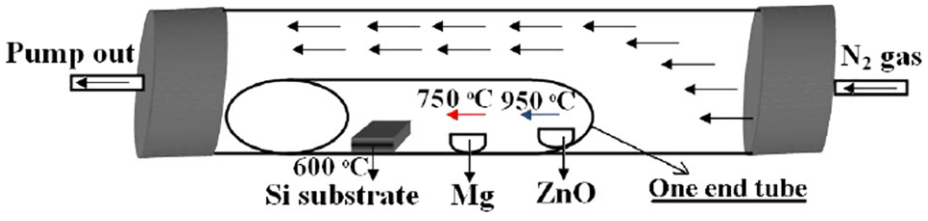

Fig. 1. Schematic of set-up that used for growth of $Zn_{1-x}Mg_xO$ and ZnO nanowires.

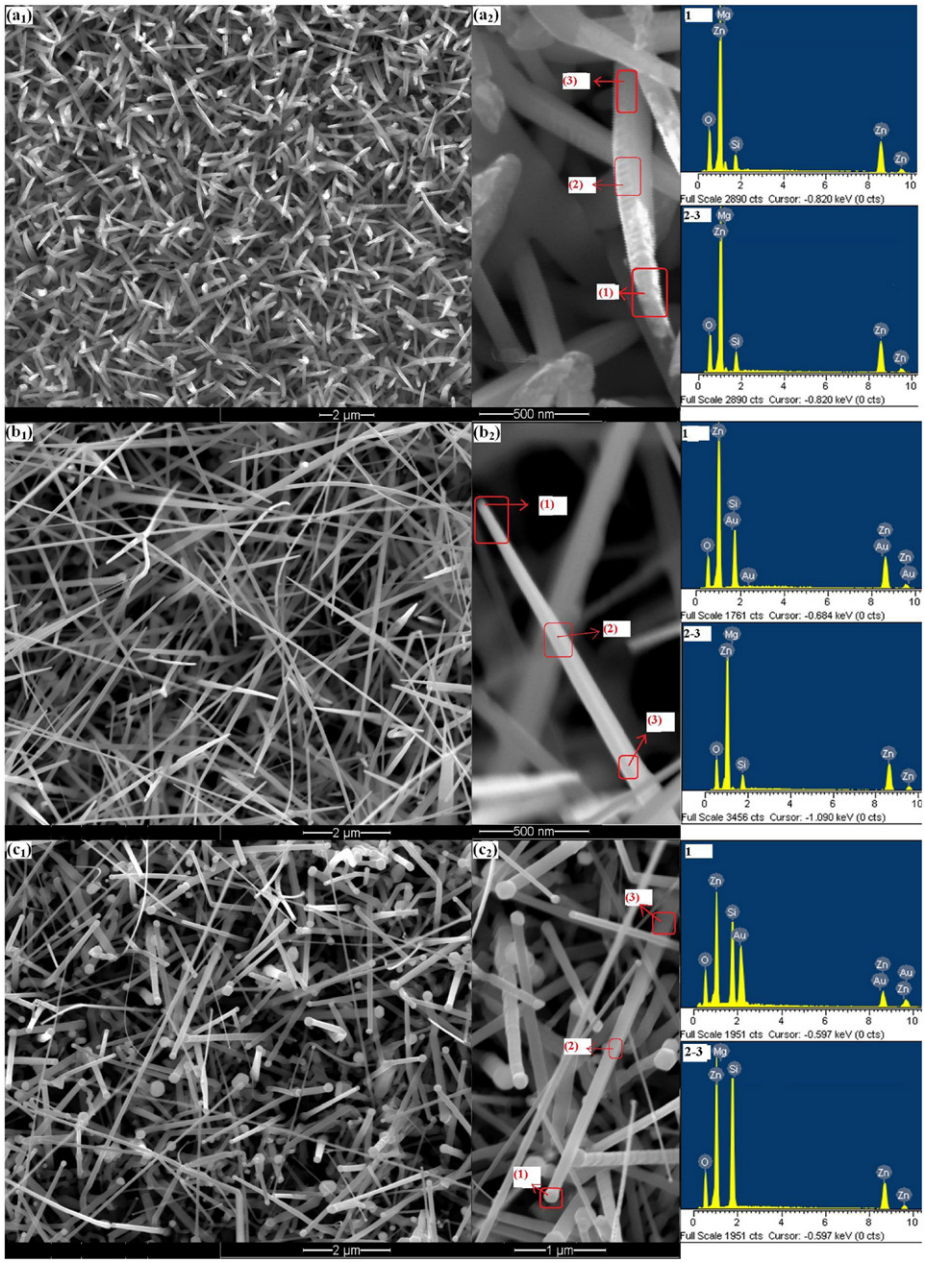

Fig. 2. Low-magnification of FESEM images of the $Zn_{1-x}Mg_xO$ nanowires that were grown on the (a_1) catalyst-free substrate, (b_1) substrate coated with 10-nm-thick Au film, and (c_1) substrate coated with 30-nm-thick Au film. (a_2–c_2) High-magnification of FESEM images of the $Zn_{1-x}Mg_xO$ nanowires with EDX spectra taken from different places along individual nanowires.

Table 1
Average Mg content in the $Zn_{1-x}Mg_xO$ nanowires grown on the various substrates and the Mg content at different places of a single nanowire.

Positions at the single nanowire	At the tip (%)	In the middle (%)	At the bottom (%)	Average (at%)
Sample a (without Au): Mg (at%)	8.4	4.3	3.1	5.2
Sample b (with 10 nm Au): Mg (at%)	0	3.8	3.0	2.5
Sample c (with 30 nm Au): Mg (at%)	0	3.5	3.2	2.4

Mg content and distribution are not affected by the increased gold film thickness (Table 1).

To better understand the growth process of $Zn_{1-x}Mg_xO$ nanowires using this set-up, pure ZnO nanowires were also grown (sample (d)) under the same conditions on the catalyst-free substrate (Fig. 3). Unlike the $Zn_{1-x}Mg_xO$ nanowires, the pure ZnO nanowires are not tapered, and they possess a uniform diameter of about 90 nm on average. Because no catalyst is used in the growth of the ZnO nanowires in this study, the VLS mechanism cannot be responsible for their growth. The absence of detectable catalyst particles at the ZnO nanowire tips supports this statement. It appears that the growth of the straight ZnO nanowires reported here occurs via a vapor–solid (VS) mechanism [28]. In addition, it can be clearly observed that the pure ZnO

nanowires have a hexagonal face at the tips and the majority of them are perpendicular to the substrate. In fact, the growth direction of the pure ZnO nanowires is along the *c*-axis.

Based on these results, the growth mechanism of $Zn_{1-x}Mg_xO$ nanowires can be tentatively proposed in this set-up. It is known that diffusion will occur even if the total pressure is uniform, as long as there is a spatial difference in the chemical potential, normally represented by differences in concentration or partial pressure, of the compounds of a gas mixture [29]. The fundamental equation used to describe one-dimensional diffusion of a gas is Fick's first law. According to Fick's law, the diffusion flux is

$$J = -D\left(\frac{dN}{dx}\right) \quad (1)$$

where J is the net flux of vapors (per unit area per unit time), D is the diffusion constant, and (dN/dx) is the concentration gradient of the vapors along the propagation direction (x) [30]. This means that the diffusion will always propagate toward the region with a lower concentration. Based on these reasons, Mg and ZnO vapors can propagate toward the substrate in our configuration (Fig. 1). But the Mg vapors reach the substrate sooner than the ZnO vapors, due to the lower melting point of Mg in comparison to ZnO. Additionally, the Mg boat is closer to the substrate than the ZnO boat (Fig. 1). When the Mg vapors reach the substrate that is placed at 600 °C, they condense and form ideal nucleation sites for the absorption of ZnO vapors on the catalyst-free Si substrate. Actually Mg droplets could act in a self-catalyst role for the growth of $Zn_{1-x}Mg_xO$ nanowires (Fig. 4a). Therefore, the $Zn_{1-x}Mg_xO$ nanowires grown on the catalyst-free substrate could also be controlled by the VLS mechanism. Thereby, the vapors of ZnO_x were absorbed by the self-catalyst, reached saturation, and then were finally solidified. Additionally, the change in the diameter of the nanowires during growth is due to the change in the droplet size of the self-catalyst. In fact, during the growth process, the Mg catalyst diffuses into the nanowires. Since the nanowire diameter size is determined by the catalyst size within the framework of the VLS mechanism, such catalyst diffusion causes a change in the nanowire diameter. This behavior can be supported by the changing Mg content along the nanowire axis (Table 1, sample (a)). Such a mechanism can act in the growth of the other samples (b,c), which were grown with a gold catalyst. The only difference between these samples is the initial droplets. In addition, this theory may be supported by the different shapes of these nanowires, because it is known that the shape of a nanowire is also dependent on its initial site: (1) sample (a), the nanowires have a cubic shape according to the cubic structures of Mg (Fig. 4a); and (2) samples (b,c), the nanowires have followed the spherical shape of the gold sites (Fig. 4b and c). It can be seen that the pure ZnO nanowires have a uniform diameter along their *c*-axis and that no catalyst particles are detected on the pure ZnO nanowire tips (Fig. 4d). A comparison between these four samples shows that the catalyst has a significant role in the formation of the different shapes. Two key questions here are as follows: (1) If a large electronegativity difference is necessary for the formation of the $Zn_{1-x}Mg_xO$ nanowires [26], how is Mg doped without using the gold catalyst in the case of the catalyst-free substrate? (2) Why is the Mg content in the $Zn_{1-x}Mg_xO$ nanowires grown on the catalyst-free substrate more than that of the other $Zn_{1-x}Mg_xO$ nanowires? Based on our previous experiments and other reports of Mg doping in ZnO, no $Zn_{1-x}Mg_xO$ nanowires have been formed by the thermal evaporation method without using Au catalysts. In fact, when Mg element is used as a doping material in a usual furnace tube (open tube), the Mg concentration in the atmosphere of the tube is very low. Therefore, in this condition, the electronegativity difference between the vapor particles and substrate can be important. On the other hand, if the Mg concentration in the furnace is increased, then the electronegativity difference is not an important factor, because the high concentration of Mg in this set-up may adjust for the small electronegativity difference. Thus, the modified thermal evaporation set-up caused the Mg concentration as an impurity in the tube to increase and Mg was doped in the ZnO without using Au. Mg droplets at the tip of the nanowires can also absorb a greater amount of Mg vapor in comparison to a gold droplet.

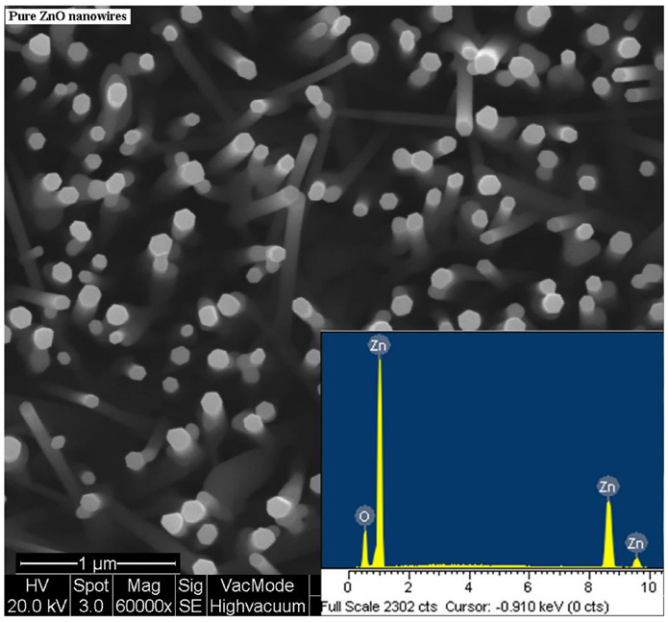

Fig. 3. FESEM image and EDX spectrum of the pure ZnO nanowires that grown on the catalyst-free substrate.

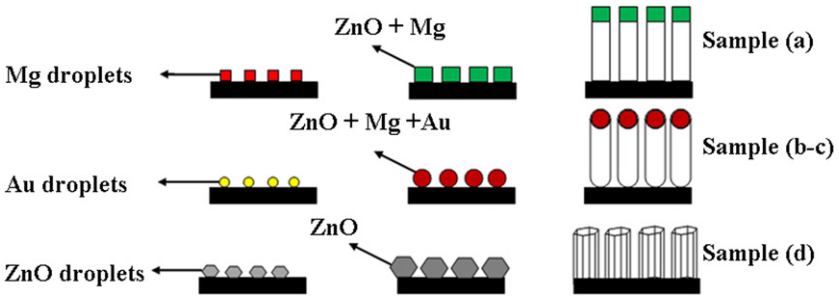

Fig. 4. Schematic of $Zn_{1-x}Mg_xO$ and ZnO nanowires formation on various substrates.

Fig. 5 shows XRD patterns for the $Zn_{1-x}Mg_xO$ (a–c) and pure ZnO (d) nanowires. The XRD patterns in Fig. 5 agree with the standard card of bulk ZnO with a hexagonal structure (JCDPDS no. 800075). No peaks from Zn, Mg, or other impurities are visible, except for sample (c), which shows an additional peak that corresponds to the Au(111) catalyst. The peak of Au appears in sample (c) because all nanowires in this sample have gold caps on their tips. The ionic radius of the substitute Mg^{2+} (r^{2+}_{Mg}=0.057 nm) is smaller than that of Zn^{2+} (r^{2+}_{Zn}=0.06 nm). Thus, doping with Mg causes a slight shift of the (002) XRD peaks toward higher diffraction angles. The extent of these shifts is dependent on the Mg content in the nanowires. Therefore, the (002) peak of sample (a) exhibits a larger shift in comparison to that of the other nanowires. These shifts are shown in the inset of Fig. 5.

PL studies are powerful methods for investigating impurity doping in ZnO nanostructures, because doped ZnO nanostructures are expected to have different optoelectronic properties in comparison to pure ZnO nanostructures. Fig. 6 shows the room temperature PL spectra of the $Zn_{1-x}Mg_xO$ (a–c) and pure ZnO (d) nanowires. All of the PL spectra show a strong peak in the ultraviolet (UV) region and negligible green emission (deep-level emission) peaks in the visible region, except for sample (c), which shows a slightly stronger green emission peak in comparison to the other nanowires. Compared with the pure ZnO nanowires (sample (d)), all of the $Zn_{1-x}Mg_xO$ samples show an obvious blue-shift in the UV emission. The blue-shift in the UV emission is believed to be a result of the Burstein–Moss effect due to Mg doping in the ZnO nanowires [31]. As the concentration of Mg increases, the blue-shift of the UV peak also increases. Particularly, for sample (a), which has a higher Mg content than the other $Zn_{1-x}Mg_xO$ nanowires, the UV emission is blue-shifted to 361 nm from 384 nm, due to the modulation of the band-gap caused by Mg substitution. Comparing these results with our previous results, the nanowires grown in the modified set-up show greater optical efficiency.

Raman spectroscopy is an effective technique for estimating the crystallinity of materials. According to the group theory, single crystalline ZnO belongs to the C^4_{6V} space group having two formula units per primitive cell and eight sets of optical phonon modes at the Γ point of the Brillouin zone, classified as $A_1+E_1+2E_2$ modes (Raman active), $2B_1$ modes (Raman silent), and A_1+E_1 modes (infrared active). The E_1 mode is a polar mode and is split into transverse optical (TO), and longitudinal optical (LO) branches. The Raman spectra for the $Zn_{1-x}Mg_xO$ (samples (a)–(c)) and pure ZnO (sample (d)) nanowires are presented in Fig. 7. As shown in Fig. 7, the Raman spectra of all of the nanowires show a sharp, strong, and dominant peak at 437 cm^{-1} corresponding to the E_2(high) mode of the Raman active mode, a characteristic peak for the wurtzite hexagonal phase of ZnO. A weak peak at 579 cm^{-1} corresponding to E_1(LO) is indicated for the $Zn_{1-x}Mg_xO$ nanowires that were grown on the substrates coated with Au. The E_1(LO) mode is associated with impurities and formation defects such oxygen vacancies [32]. Therefore, the appearance of the E_1(LO) mode for samples (b) and (c) indicates a

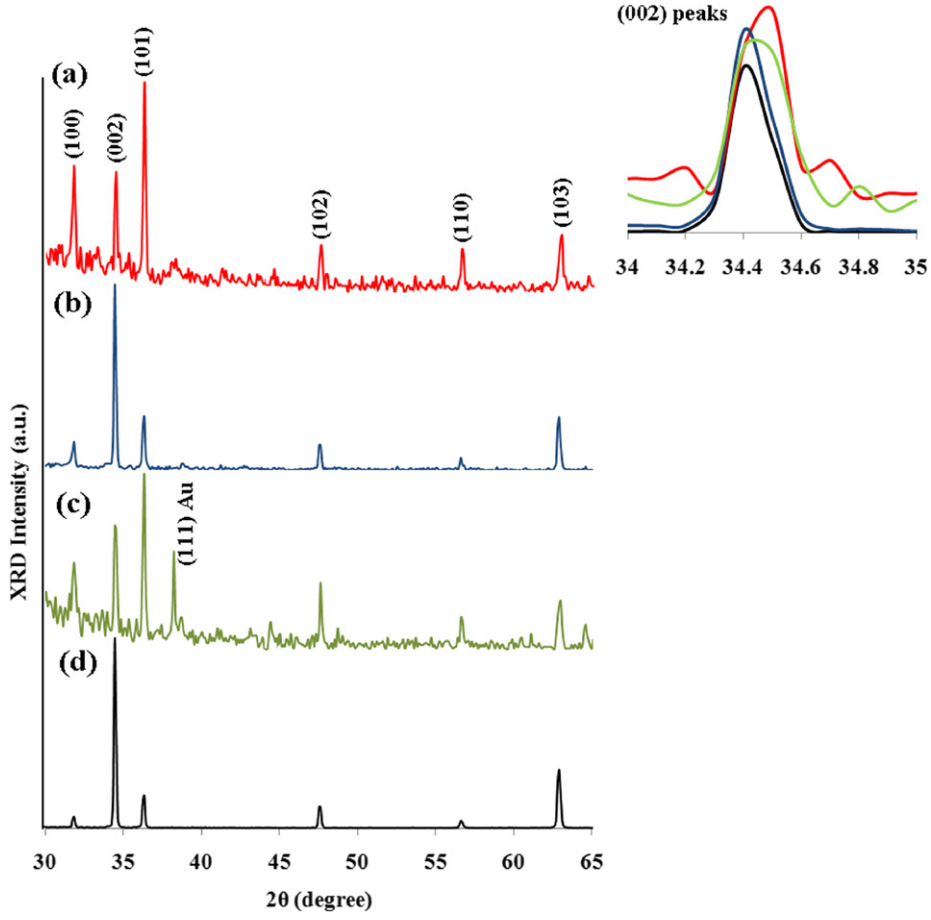

Fig. 5. XRD patterns of the $Zn_{1-x}Mg_xO$ nanowires grown on the (a) catalyst-free substrate, (b) substrate coated with 10-nm-thick Au film, (c) substrate coated with 30-nm-thick Au film, and (d) pure ZnO nanowires. No peaks from impurities are detected, except for sample (c), which shows an additional peak that corresponds to the Au(111) catalyst. The inset shows the shifts of (002) peaks of the $Zn_{1-x}Mg_xO$ nanowires in comparison to the (002) peak of the pure ZnO nanowires.

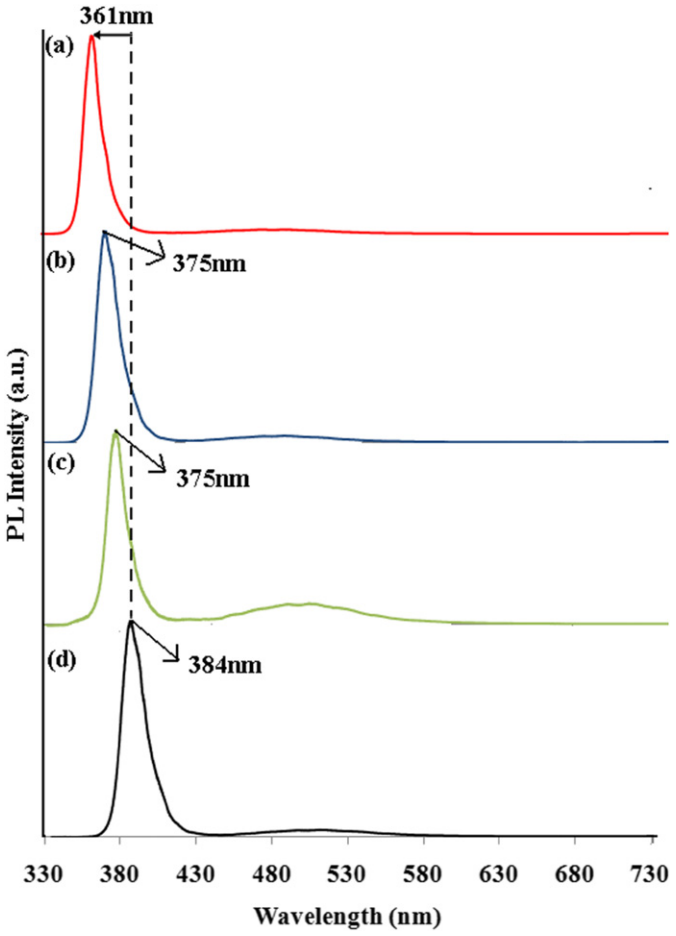

Fig. 6. PL spectra of the $Zn_{1-x}Mg_xO$ nanowires grown on the (a) catalyst-free substrate, (b) substrate coated with 10-nm-thick Au film, (c) substrate coated with 30-nm-thick Au film, and (d) pure ZnO nanowires. All of the $Zn_{1-x}Mg_xO$ samples show an obvious blue-shift in the UV emission in comparison to the pure ZnO nanowires.

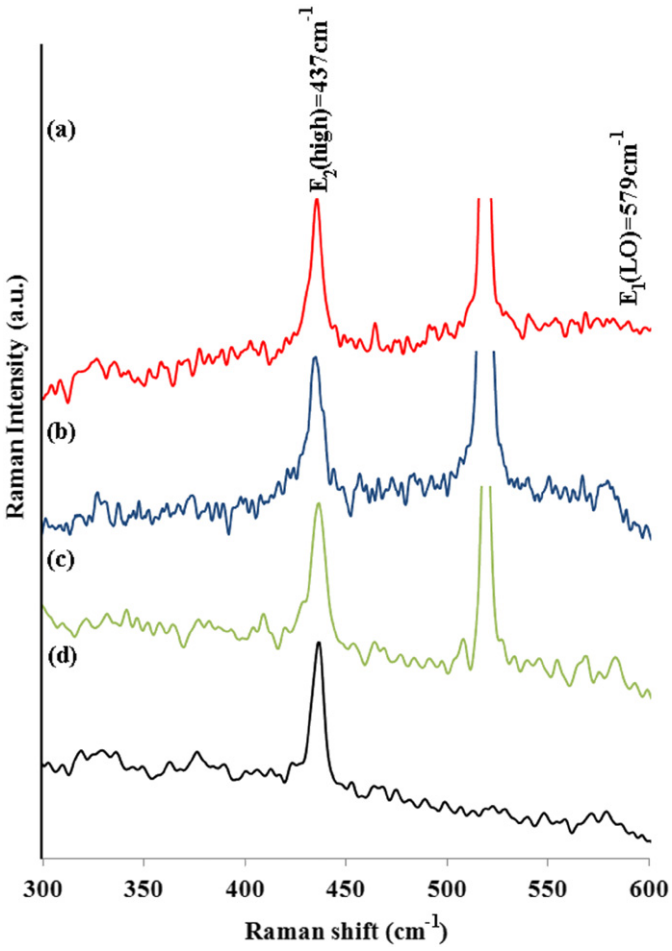

Fig. 7. Raman spectra of the $Zn_{1-x}Mg_xO$ nanowires grown on the (a) catalyst-free substrate, (b) substrate coated with 10-nm-thick Au film, (c) substrate coated with 30-nm-thick Au film, and (d) pure ZnO nanowires. All of the nanowires show a sharp, strong, and dominant peak at 437 cm^{-1} corresponding to the E_2 (high) mode of the Raman active mode, a characteristic peak for the wurtzite hexagonal phase of ZnO.

lower crystalline quality and higher oxygen vacancy of the $Zn_{1-x}Mg_xO$ nanowires grown on the substrates coated with Au films in comparison to the $Zn_{1-x}Mg_xO$ and pure ZnO nanowires grown on the catalyst-free substrates. Therefore, the existence of a catalyst such as Au in the nanowire tips may cause the decreased crystalline quality of the ZnO nanowires.

4. Conclusions

$Zn_{1-x}Mg_xO$ nanowires were successfully deposited on Si substrates using a modified thermal evaporation method, with and without the use of a gold catalyst. A one-ended quartz tube was used as a tool to modify the thermal evaporation process and caused the concentration of Mg to increase in the tube. The EDX results showed that the distribution of Mg in the $Zn_{1-x}Mg_xO$ nanowires grown with the catalyst-free substrate was dramatically different in comparison to that of the $Zn_{1-x}Mg_xO$ nanowires grown on the substrates coated with Au. Additionally, the Mg content and distribution were not affected by the increase of gold film thickness for the $Zn_{1-x}Mg_xO$ nanowires, which were grown on the substrates coated with Au. The PL and Raman measurements exhibited that the $Zn_{1-x}Mg_xO$ nanowires grown on the catalyst-free substrate have a higher optical efficiency and crystalline quality than the other $Zn_{1-x}Mg_xO$ nanowires.

Acknowledgments

This work was supported by the University of Malaya through Grant no. PS 199/2008. B.R. Yousefi gratefully acknowledges the University of Malaya for its fellowship. In addition, R. Yousefi would like to dedicate this paper to his late supervisor (Associated Professor Dr. Burhanuddin Kamaluddin) who passed away during this research. Also, the authors acknowledge Professor Yoke Khin Yap from Michigan Technology, USA for his constructive advice.

References

[1] M.H. Huang, S. Mao, H. Yan, Y. Wu, H. Kind, E. Weber, R. Russo, P. Yang, Science 292 (2002) 1897–1899.
[2] J.P. Kar, M.C. Jeong, W.K. Lee, J.M. Myoung, Mater. Sci. Eng. B 147 (2008) 74–78.
[3] W. Liu, S. Gu, S. Zhu, J. Ye, F. Qin, S. Liu, X. Zhou, L. Hu, R. Zhang, Y. Shi, Y. Zheng, J. Cryst. Growth 277 (2005) 416–421.
[4] D.K. Hwang, M.C. Jeong, J.M. Myoung, Appl. Surf. Sci. 225 (2004) 217–222.
[5] R. Kling, C. Kirchner, Th. Gruber, F. Reuss, A. Waag, Nanotechnology 15 (2004) 1043–1046.
[6] W.I. Park, S.J. An, J.L. Yang, G.C. Yi, S. Hong, T. Joo, M. Kim, J. Phys. Chem. B 108 (2004) 15457–15460.
[7] A.L. Yang, H.Y. Wei, X.L. Liu, H.P. Song, G.L. Zheng, Y. Guo, C.M. Jiao, S.Y. Yang, Q.S. Zhu, Z.G. Wang, J. Cryst. Growth 311 (2009) 278–281.
[8] Y.J. Zeng, Z.Z. Ye, F. Liu, D.Y. Li, Y.F. Lu, W. Jeager, H.P. He, L.P. Zhu, J.Y. Huang, B.H. Zhao, Cryst. Growth Des. 9 (2009) 263–266.

[9] W.I. Park, J. Yoo, D.W. Kim, G.C. Yi, M. Kim, J. Phys. Chem. B 110 (2006) 1516–1519.
[10] J.R. Wang, Y.Z. Zhang, Z.Z. Ye, J.G. Lu, H.P. He, Y.J. Zeng, Q.B. Ma, J.Y. Huang, L.P. Zhu, Y.Z. Wu, Y.F. Yang, L. Goang, J. Appl. Phys. 104 (2008) 103507.
[11] A.L. Yang, H.Y. Wei, X.L. Liu, H.P. Song, H.B. Fan, P.F. Zhang, G.L. Zheng, S.Y. Yang, Q.S. Zhu, Z.G. Wang, J. Phys. D.: Appl. Phys. 41 (2008) 205416.
[12] M. Lorenz, E.M. Kaidashev, A. Rahm, Th. Nobis, J. Lenzner, G. Wagner, D. Spemann, H. Hochmuth, M. Grundmann, Appl. Phys. Lett. 86 (2005) 143113.
[13] C. Czekalla, J. Guinard, C. Hanisch, B.Q. Cao, E.M. Kaidashev, N. Boukos, A. Travlos, J. Renard, B. Gayral, D. Le Dang, M. Lorenz, M. Grundmann, Nanotechnology 19 (2008) 115202.
[14] Y.Z. Zhang, J.G. Lu, Z.Z. Ye, Y.J. Zeng, L.P. Zhu, J.Y. Huang, J. Phys. D: Appl. Phys. 40 (2007) 3490–3493.
[15] F. Wang, C. Zhao, B. Liu, S. Yuan, J. Phys. D: Appl. Phys. 42 (2009) 115411.
[16] M. Zhi, L. Zhu, Z. Ye, F. Wang, B. Zhao, J. Phys. Chem. B 109 (2005) 23930–23934.
[17] L. Zhu, M. Zhi, Z. Ye, B. Zhao, Appl. Phys. Lett. 88 (2006) 113106.
[18] G. Wang, Z. Ye, H. He, H. Tang, J. Li, J. Phys. D: Appl. Phys. 40 (2007) 5287–5290.
[19] Q. Wei, M. Li, Z. Yang, L. Cao, W. Zhang, H. Liang, Acta Phys. Chem. Sin. 24 (2008) 793–798.
[20] H.C. Hsu, C.Y. Wu, H.M. Cheng, W.F. Hsieh, Appl. Phys. Lett. 89 (2006) 013101.
[21] H. Tang, H. He, L. Zhu, Z. Ye, M. Zhi, F. Yang, B. Zhao, J. Phys. D: Appl. Phys. 39 (2006) 3764–3768.
[22] C.J. Pan, H.C. Hsu, H.M. Cheng, C.Y. Wu, W.F. Hsieh, J. Solid State Chem. 180 (2007) 1188–1192.
[23] M.X. Qiu, Z.Z. Ye, H.P. He, Y.Z. Zhang, H.P. Tang, X.Q. Gu, L.P. Zhu, B.H. Zhao, J.Y. Huang, J.G. Lu, J. Phys. D: Appl. Phys. 41 (2008) 085109.
[24] C.H. Ahn, S.K. Mohanta, B.H. Kong, H.K. Cho, J. Phys. D: Appl. Phys. 42 (2009) 115106.
[25] R. Yousefi, B. Kamaluddin, Appl. Surf. Sci. 256 (2009) 329.
[26] S.N. Mohammad, Nano Lett. 8 (2008) 1532–1538.
[27] X. Wang, C.J. Summers, Z.L. Wang, Nano Lett. 4 (2004) 423–426.
[28] Z.L. Wang, J. Phys.: Condens. Matter 16 (2004) R829–R858.
[29] C. Kittel, in: Thermal Physics, first ed., John Wily & Sons, Inc., New York, 1969.
[30] C. Kittel, in: Introduction to Solid State Physics, sixth ed., Wiley, New York, 1986.
[31] K.J. Kim, Y.R. Park, Appl. Phys. Lett. 78 (2001) 475–477.
[32] A. Umar, S.H. Kim, Y.S. Lee, K.S. Nahm, Y.B. Hahn, J. Cryst. Growth 282 (2005) 131–136.